

ANALYSIS OF A DEGENERATE BIOFILM MODEL WITH A NUTRIENT TAXIS TERM

HERMANN J. EBERL

Dept. Mathematics and Statistics, University of Guelph
Guelph, ON, N1G 2W1, Canada

MESSOUD A. EFENDIEV

Helmholtz Zentrum München, Institute of Computational Biology
Ingolstädter Landstrasse 1, D-85764 Neuherberg, Germany

DARIUSZ WRZOSEK

Inst. Applied Mathematics and Mechanics, University of Warsaw
Banacha 2, 02-097 Warszawa, Poland

ANNA ZHIGUN

Centre for Mathematical Sciences, Technical University of Munich
Boltzmannstr. 3, 85748 Garching, Germany

ABSTRACT. We introduce and analyze a prototype model for chemotactic effects in biofilm formation. The model is a system of quasilinear parabolic equations into which two thresholds are built in. One occurs at zero cell density level, the second one is related to the maximal density which the cells cannot exceed. Accordingly, both diffusion and taxis terms have degenerate or singular parts. This model extends a previously introduced degenerate biofilm model by combining it with a chemotaxis equation. We give conditions for existence and uniqueness of weak solutions and illustrate the model behavior in numerical simulations.

1. Introduction. Bacterial biofilms are microbial depositions on immersed biotic or abiotic surfaces. Cells attach to the surface and start producing extracellular polymeric substances (EPS, exopolysaccharides) in which they are themselves embedded. Protected by this gel-like layer, the bacteria form vivid colonies. Biofilms are ubiquitous. They can be found virtually everywhere, where the environmental conditions permit microbial growth. This includes medical and industrial systems, as well as natural surfaces such as plant roots, or engineered systems which are sometimes designed based on biofilm processes, for example in wastewater treatment.

It has been suggested that biofilm formation involves chemotaxis [26], i.e. the directed movement of cells in response to chemical gradients. Other authors have pointed out that this might in particular be important for plant associated biofilms and the colonization of biotic surfaces, provided the environmental conditions are suitable [21]. However, the experimental evidence for the role of chemotaxis in

2010 *Mathematics Subject Classification.* Primary: 35K55, 35K65, 34B15; Secondary: 92C17, 92D25.

Key words and phrases. Chemotaxis, biofilm, degenerate diffusion, fast diffusion, singular quasilinear parabolic equation, compactness method.

biofilm formation seems meager, and several experimental studies remained inconclusive [17]. An interesting study of chemotaxis in biofilm formation is [37], in which it was found that *Bacillus amyloliquefaciens* shows chemotactic response in the biofilm colonization of soybean seeds, but not in the colonization of soybean roots. This suggests that chemotaxis is not a ubiquitous and generally required mechanism in early stages of biofilm formation but rather a secondary mechanism that can play a role in certain systems. Moreover, the study suggests also that it is not only a question of the microbial species and of the attractant but also of the environmental context. With current experimental evidence inconclusive there is the hope that eventually mathematical modeling might be able to guide further laboratory efforts. Both biofilm modeling and chemotaxis modeling have matured in recent decades as sub-disciplines of mathematical biology. This paper is intended as a first step toward combining both by providing a general mathematical framework to model such biofilm- taxis systems.

The model we investigate here mathematically describes changes in biomass density in early stages of biofilm formation when the cells respond to the gradient of a growth controlling substrate, in our case a nutrient. As is common practice in biofilm modelling, we subsume in the ‘biomass’ both, cells and EPS. We study the well-posedness of the following singular-degenerate parabolic system describing changes in the local density of a biofilm. The model extends the previous biofilm model proposed in [7] and analysed in [10] by taking into account nutrient taxis understood as the movement of cells up a nutrient concentration gradient.

Denoting by M the biomass density and by S the substrate or nutrient concentration, we consider

$$\partial_t S = d_1 \Delta S - F(S, M), \quad (1)$$

$$\partial_t M = \nabla \cdot \left(d_{21} \frac{M^b}{(1-M)^a} \nabla M - d_{22} M^d (1-M)^c \nabla S \right) + G(S, M), \quad (2)$$

satisfied in $(0, +\infty) \times \Omega$, with initial conditions

$$(S, M)(0) = (S_0, M_0) \quad \text{in } \Omega, \quad (3)$$

where Ω is a bounded open subset of \mathbb{R}^N with smooth boundary $\partial\Omega$. On the boundary, we assume for our analysis a fixed bulk concentration of nutrient and zero density of biomass;

$$S = 1, M = 0, \quad \text{on } (0, +\infty) \times \partial\Omega. \quad (4)$$

The function $F = F(S, M)$ describes the consumption rate of the nutrient and $G = G(S, M)$ is the growth rate of the biofilm. The values of positive parameters a, b, c, d will be specified later; d_1 is the diffusion coefficient for nutrient, and d_{21}, d_{22} are motility coefficients for biomass due to diffusion and chemotaxis, respectively.

The basic assumption made here is the existence of a threshold value for the cell density which corresponds to a tight packing state normalized to $M = 1$. In other words, cells cannot accumulate without bound at a given point of Ω , and the corresponding volume filling effect is taken into account. Moreover, in a fully developed biofilm with $M \approx 1$, cells can be assumed to be largely immobilized in the EPS matrix and not able to respond to chemical cues. This is accounted for by turning off chemotaxis for large M in (2). The effect of the threshold cell density or a volume-filling effect has been taken into account in the modeling of chemotaxis phenomena in a class of models sharing some common features with the present one. We refer the reader to [23] and to the survey of corresponding mathematical results

[35]. We would also like to point out a recent paper [20] on a chemotaxis model where singular diffusion of cells appears in the macroscopic limit of a microscopic cellular Potts model. A natural question for this class of models, whether the cell density initially below the threshold will attain this value eventually, was recently studied in [30, 31].

We assume the following structural assumptions on the functions $F, G \in \mathcal{C}^2(\mathbb{R}^2)$.

$$F(0, M) \geq 0 \quad F(1, M) \geq 0 \quad \text{for all } M \geq 0, \quad (5)$$

$$F(S, M) = f_1(S) + Mf_2(S), \quad f_1(0) = f_2(0) = 0 \quad (6)$$

where $f_1, f_2 \in \mathcal{C}^2(\mathbb{R})$ are some functions. We next assume that there exists a function $g \in \mathcal{C}^2(\mathbb{R})$ such that

$$G(S, M) = g(S)M^\alpha(1 - M)^\beta, \quad \alpha, \beta > 0. \quad (7)$$

We note that for the existence of solutions only (5), (7) are required and (6) is additionally assumed for the uniqueness of solutions.

The primary example of functions satisfying the above assumptions is the Monod's function for nutrient up-take

$$F(S, M) = \frac{k_1 SM}{k_2 + S}, \quad k_1, k_2 > 0, \quad (8)$$

and logistic-like growth functions for biomass growth

$$G(S, M) = \frac{k_3 S}{k_2 + S} M M^{\alpha-1} (1 - M)^\beta, \quad k_3 > 0, \quad (9)$$

in which the growth rate is proportional to the consumption rate F . Notice that due to the high density stress, the cell proliferation drops to zero at $M = 1$ even for high food concentration. We would like to underline at this point that the shape of the reaction terms in both equations is forced by the analysis of the well-posedness of the system and, in particular, the uniqueness of solutions. The specific reaction terms deviate from standard growth kinetics used in most biofilm studies. The form of the reaction term G reflects critical phenomena which take place when the diffusion degenerates at $M = 0$ and when it becomes singular at $M = 1$. The important case $\alpha > 1$ leads to a delay of biomass growth, especially during early stages for small $0 < M \ll 1$. This can be understood as mimicking a 'lag-phase', which is commonly observed in the onset of bacterial growth due to physiological adaptation. Note that most biofilm modeling studies in the literature focus on the long term evolution of a mature biofilm, which corresponds in our modeling framework to $M \approx 1$ almost everywhere in the biofilm. In fact, some biofilm models explicitly assume $M \equiv 1$ [5]. In this case it is not required to account for the initial lag-phase in bacterial growth. In a study that focuses on early stages and onset of biofilm growth, however, including lag-effects, if only qualitatively, seems justified and warranted. Our model assumes that during this lag-phase, nutrient consumption is proportionally higher than growth of new biomass due to resources required for cell repair and adaptation. We point out that in the predictive microbiology modelling literature, lag-phase models are usually more involved, often including an extra dependent variable that describes in some sense the physiological state of the cells, see [13, 14] for some variants and discussion.

Note further that the growth rate G vanishes for $M = 1$, but the substrate consumption rate does not. This mimics that nutrients are required for cell maintenance even if no net growth takes place. The variables M and S are dimensionless.

S is scaled with respect to the bulk concentration, and M is scaled relative to the maximum biomass density, i.e. it can also be understood as the volume fraction locally occupied by the biofilm. We make the following assumptions on the initial data:

$$(S_0, M_0) \in L^\infty(\Omega; \mathbb{R}^2) \quad \text{with} \quad 0 \leq S_0, M_0 \leq 1 \quad \text{a.e. in } \Omega. \quad (10)$$

To shorten the notation, we define

$$D(M) = d_{21} M^b (1 - M)^{-a},$$

and introduce

$$\mathcal{D}(r) := \int_0^r D(s) ds, \quad r \in [0, 1].$$

Because of degeneracy and singularity in the diffusion term of (2), we shall consider weak solutions to (1)-(3). A similar concept of weak solution was already introduced in [18] for chemotaxis system with degenerate diffusion and volume filling effect. We assume from now on that $a \in (0, 1)$.

Definition 1.1. A weak solution to (1)-(4) is a pair (S, M) of functions such that, for each $T > 0$,

$$0 \leq S(t, x), M(t, x) \leq 1, \quad \text{a.e. in } (0, T) \times \Omega,$$

$$S \in C([0, T], L^2(\Omega)) \cap W_{loc}^{1,2}((0, T); L^2(\Omega)) \cap L_{loc}^2((0, T); H^2(\Omega)), \quad (11)$$

$$M \in L^\infty((0, T) \times \Omega) \cap \mathcal{C}_w([0, T]; L^2(\Omega)), \quad \mathcal{D}(M) \in L^2(0, T; H^1(\Omega)), \quad (12)$$

$$S(0) = S_0, \quad M(0) = M_0$$

and (S, M) satisfies

$$\partial_t S = d_1 \Delta S - F(S, M) \quad \text{a.e. in } (0, T) \times \Omega, \quad (13)$$

$$\int_0^T \langle \partial_t M, \psi \rangle dt + \int_0^T \int_\Omega (\nabla \mathcal{D}(M) - d_{22} M^d (1 - M)^c \nabla S) \cdot \nabla \psi \, dx dt \quad (14)$$

$$= \int_0^T \int_\Omega G(S, M) \psi \, dx dt,$$

$$S = 1 \quad \text{a.e. on } (0, T) \times \partial\Omega,$$

for each $t \in [0, T]$ and $\psi \in L^2(0, T; H_0^1(\Omega))$.

Here we denote by $\langle \cdot, \cdot \rangle$ the duality pairing between $H_0^1(\Omega)$ and $H^{-1}(\Omega)$, and $\mathcal{C}_w([0, T]; L^2(\Omega))$ denotes the set of functions from $[0, T]$ in $L^2(\Omega)$ which are continuous in the weak topology of $L^2(\Omega)$.

Theorem 1.2. Assume that (S_0, M_0) satisfies (10) and (5), (7) hold. If

$$a \in (0, 1), \quad b > 0, \quad \min\{c, d, \alpha, \beta\} \geq 1,$$

then there exists at least one weak solution (S, M) to (1)-(3) in the sense of Definition 1.1.

It is worth noticing that the assumption $a \in (0, 1)$ corresponds to the so called fast diffusion according to Aronson's classification (cf. [3]) whereas the density-dependent biofilm model as originally introduced and studied in [7, 10] used a super-diffusion singularity instead.

The uniqueness of solutions demands both more regularity of the first component S than that in Definition 1.1 and an additional structural assumption on F .

Theorem 1.3. *Assume in addition to the assumptions of Theorem 1.2 that (6) holds and $S_0 - 1 \in W^{2,p}(\Omega) \cap H_0^1(\Omega)$ for some $p > \max(2, N)$. If*

$$a \in (0, 1), \quad b > 0, \quad \min\{c, \beta\} \geq 1 - \frac{a}{2}, \quad \min\{d, \alpha\} \geq 1 + \frac{b}{2},$$

then the weak solution to (1)-(3) is uniquely determined.

We would like to point out that the results are closely related to earlier works [11, 12, 18, 34] on systems of similar structure. The proofs of Theorem 1.2 and Theorem 1.3 are given in Section 2.

At the end of the introduction, we present a derivation of model (1)-(2) based on a hydrodynamical approach which was applied for the first time to the chemotaxis equations in [16], and then generalized for the volume filling chemotaxis model in [33], and independently for biofilm models in [15]. The population of cells is treated now as a non-viscous fluid with density M and velocity \mathbf{v} , which satisfy Euler equations. First we assume that the nutrient concentration $S(t, x)$ is given and the local rate of production of cells with density M is equal to $G(S, M)$. Then mass balance and momentum equations read

$$\begin{aligned} \partial_t M + \nabla \cdot (M\mathbf{v}) &= G(S, M), \\ M(\partial_t \mathbf{v} + \mathbf{v} \cdot \nabla \mathbf{v}) &= -\nabla p + \Phi(S, M, \mathbf{v}), \end{aligned} \quad (15)$$

with the density-dependent pressure $p = p(M)$ and the force

$$\Phi = \mu \nabla S - \beta(M)\mathbf{v}$$

composed of a chemotactic part oriented towards the gradient of nutrient S and a density dependent resistive force $\beta(M)\mathbf{v}$ which subsumes all factors moderating cell movement including kinematic friction. Then, assuming that inertial force is negligible for the description of cells movement, we obtain the Darcy like equation

$$\mu \nabla S - \nabla p(M) - \beta(M)\mathbf{v} = 0.$$

Using (15), we arrive at

$$\partial_t M = \nabla \cdot \left(\frac{Mp'(M)}{\beta(M)} \nabla M - \frac{\mu M}{\beta(M)} \nabla S \right) + G(S, M).$$

Finally, setting $\mu = d_{22}$ and

$$\beta(M) = M^{-(d-1)}(1-M)^{-c} \quad \text{and} \quad p'(M) = d_{21}M^{b-d}(1-M)^{-(a+c)},$$

we formally obtain (2).

2. Well-posedness.

2.1. Existence. To prove Theorem 1.2, we first consider a suitable regularized problem and then use the compactness method. The regularization is adapted from [11, 28].

Proof of Theorem 1.2. For $\varepsilon \in (0, 1/4)$, we consider

$$\partial_t S_\varepsilon = d_1 \Delta S_\varepsilon - F(S_\varepsilon)M_\varepsilon, \quad (16)$$

$$\begin{aligned} \partial_t M_\varepsilon &= \nabla \cdot \left(\frac{d_{21}(M_\varepsilon + \varepsilon)^b}{(1 - M_\varepsilon)^a} \nabla M_\varepsilon \right) \\ &\quad - d_{22}(M_\varepsilon + \varepsilon)^{d-1} M_\varepsilon (1 - \varepsilon - M_\varepsilon)(1 - M_\varepsilon)^{c-1} \nabla S_\varepsilon \\ &\quad + g(S_\varepsilon)(M_\varepsilon + \varepsilon)^{\alpha-1} M_\varepsilon (1 - \varepsilon - M_\varepsilon)(1 - M_\varepsilon)^{\beta-1}, \end{aligned} \quad (17)$$

satisfied in $(0, +\infty) \times \Omega$ with boundary condition (4) and initial conditions

$$(S_{0,\varepsilon}, M_{0,\varepsilon}) \in W^{1,N+1}(\Omega; \mathbb{R}^2) \quad (18)$$

satisfying

$$0 \leq S_{0,\varepsilon} \leq 1, \quad 0 \leq M_{0,\varepsilon} \leq 1 - 2\varepsilon, \quad (19)$$

$$\|M_{0,\varepsilon} - M_0\|_{L^2} + \|S_0^\varepsilon - S_0\|_{L^2} \leq \varepsilon. \quad (20)$$

Notice that there exists $\delta > 0$ such that all nonlinear terms in (16)-(17) are smooth for $M \in (-\delta, 1 - \varepsilon + \delta)$ and (16)-(17) is a regular parabolic system. The change of variables $\tilde{S}_\varepsilon = 1 - S_\varepsilon$ leads to an equivalent problem with homogeneous boundary conditions. Since (18) and (19) are satisfied, we can apply [2, Theorems 14.4 & 14.6], which entails that the corresponding initial-boundary value problem has a unique maximal classical solution $(S_\varepsilon, M_\varepsilon)$ defined on $(0, T_{\max}) \times \Omega$, for some $T_{\max} \in (0, \infty]$. We refer the reader to [18, Theorem 3] for more details on the applications of Amann's theory to the problem of well-posedness of such systems. To extend the solution for all $t \in (0, +\infty)$, we observe that the main part of the elliptic operator in (16)-(17) is upper triangular. For such systems, it is sufficient to find a uniform in time L^∞ -bound for the solution (see [2, Theorem 15.5]). First, using (5), (7), we deduce that the components of the solution are nonnegative. To prove this, we may use [8] or apply the parabolic maximum principle to each equation separately, after transforming the equation (17) into non-divergence form. This step is admissible due to the regularity of the solution and smoothness of the nonlinearities. Hence, we obtain $S_\varepsilon \geq 0, M_\varepsilon \geq 0$ on $(0, T) \times \Omega$ for any $T < T_{\max}$. By comparison with the function $S \equiv 1$, we infer that $S_\varepsilon \leq 1$. To get the upper bound on M_ε , we change variables in (17) setting $z_\varepsilon = 1 - \varepsilon - M_\varepsilon$. Then, making use of (4) and (18)-(20), we can apply similar arguments based on the maximum principle to conclude that $z_\varepsilon \geq 0$. Hence, for any $T < T_{\max}$, we have

$$0 \leq M_\varepsilon \leq 1 - \varepsilon \quad \text{on } (0, T) \times \Omega. \quad (21)$$

Thus, $(S_\varepsilon, M_\varepsilon)$ is defined globally in time.

Below we denote by $C_i, i = 1, 2, \dots$ positive constants which do not depend on $\varepsilon \in (0, 1/2)$, but may depend on the model parameters or T . It follows from the classical energy estimate for parabolic equations that for each $T > 0$ there is a positive constant $C_1(T)$ such that

$$\|S_\varepsilon\|_{L^2(0,T;H^1(\Omega))} + \|\partial_t S_\varepsilon\|_{L^2((0,T);H^{-1}(\Omega))} \leq C_1(T). \quad (22)$$

We next denote $D^\varepsilon(r) = d_2(r + \varepsilon)^b(1 - r)^{-a}$ and introduce the functions \mathcal{D}^ε and \mathcal{E}^ε defined by

$$\frac{d^2 \mathcal{E}^\varepsilon}{dr^2} = \frac{d\mathcal{D}^\varepsilon}{dr} = D^\varepsilon \quad \text{and} \quad \mathcal{E}^\varepsilon(0) = \mathcal{D}^\varepsilon(0) = 0.$$

A similar definition is used for \mathcal{E} corresponding to the case $\varepsilon = 0$. Note that for $\varepsilon \in (0, 1/4)$

$$\mathcal{D}^\varepsilon(x) \leq \mathcal{D}^{1/4}(x) \quad \text{for } x \in [0, 1], \quad (23)$$

$$\mathcal{D}^\varepsilon, \mathcal{D} \in C[0, 1],$$

$$\lim_{\varepsilon \searrow 0} \|\mathcal{D}^\varepsilon - \mathcal{D}\|_\infty = 0. \quad (24)$$

We multiply (17) by $\mathcal{D}^\varepsilon(M_\varepsilon)$ and integrate over Ω to obtain

$$\begin{aligned} & \frac{d}{dt} \int_{\Omega} \mathcal{E}^\varepsilon(M_\varepsilon) dx = \\ & - \int_{\Omega} \nabla \mathcal{D}^\varepsilon(M_\varepsilon) \left[\nabla \mathcal{D}^\varepsilon(M_\varepsilon) - d_{22}(M_\varepsilon + \varepsilon)^{d-1} M_\varepsilon (1 - \varepsilon - M_\varepsilon) (1 - M_\varepsilon)^{c-1} \nabla S_\varepsilon \right] dx \\ & - \int_{\Omega} g(S_\varepsilon) (M_\varepsilon + \varepsilon)^{\alpha-1} M_\varepsilon (1 - \varepsilon - M_\varepsilon) (1 - M_\varepsilon)^{\beta-1} \mathcal{D}^\varepsilon(M_\varepsilon) dx. \end{aligned}$$

Using Hölder's inequality as well as the L^∞ bound on M_ε and (22), we arrive at

$$\begin{aligned} & \frac{d}{dt} \int_{\Omega} \mathcal{E}^\varepsilon(M_\varepsilon) dx \leq - \|\nabla \mathcal{D}^\varepsilon(M_\varepsilon)\|_{L^2}^2 \\ & + \|d_{22}(M_\varepsilon + \varepsilon)^{d-1} M_\varepsilon (1 - \varepsilon - M_\varepsilon) (1 - M_\varepsilon)^{c-1}\|_{L^\infty(0,1)} \|\nabla \mathcal{D}^\varepsilon(M_\varepsilon)\|_{L^2} \|\nabla S_\varepsilon\|_{L^2} \\ & + \sup_{r \in [0,1]} |g(r) \mathcal{D}^\varepsilon(r)| \|(M_\varepsilon + \varepsilon)^{\alpha-1} M_\varepsilon (1 - \varepsilon - M_\varepsilon) (1 - M_\varepsilon)^{\beta-1}\|_{L^\infty} |\Omega| \\ & \leq -\frac{1}{2} \|\nabla \mathcal{D}^\varepsilon(M_\varepsilon)\|_{L^2}^2 + C_3(T), \end{aligned}$$

where (23) was also used. On integrating with respect to time, we get

$$\int_0^T \int_{\Omega} |\nabla \mathcal{D}^\varepsilon(M_\varepsilon)|^2 dx dt \leq C_4(T). \quad (25)$$

Hence,

$$\int_0^T \int_{\Omega} |\nabla \mathcal{D}(M_\varepsilon)|^2 dx dt \leq C_4(T). \quad (26)$$

Making use of (17), we deduce from (21), (22) and (25) that

$$\int_0^T \|\partial_t M_\varepsilon\|_{H^{-1}(\Omega)}^2 dt \leq C_5(T). \quad (27)$$

The estimates we have obtained so far allow us to use a weak compactness argument, which is not sufficient for passing to the limit in all the terms in the weak formulation of (17):

$$\begin{aligned} & \int_0^T \langle \partial_t M_\varepsilon, \psi \rangle dt + \int_0^T \int_{\Omega} [\nabla \mathcal{D}^\varepsilon(M_\varepsilon) \\ & - d_{22}(M_\varepsilon + \varepsilon)^{d-1} M_\varepsilon (1 - \varepsilon - M_\varepsilon) (1 - M_\varepsilon)^{c-1} \nabla S_\varepsilon] \nabla \psi dx dt \\ & = \int_0^T \int_{\Omega} g(S_\varepsilon) (M_\varepsilon + \varepsilon)^{\alpha-1} M_\varepsilon (1 - \varepsilon - M_\varepsilon) (1 - M_\varepsilon)^{\beta-1} \psi dx dt. \end{aligned} \quad (28)$$

In order to deduce the convergence of $\{M_\varepsilon\}$ almost everywhere for some subsequence, we shall first show that

$$\{\mathcal{E}(M_\varepsilon)\} \text{ is bounded in } L^2(0, T; H^1(\Omega)), \quad (29)$$

$$\{\partial_t \mathcal{E}(M_\varepsilon)\} \text{ is bounded in } L^1(0, T; W^{1,N+1}(\Omega)') \quad (30)$$

for each $T > 0$. Since $a \in (0, 1)$, both \mathcal{D} and \mathcal{E} are bounded functions and

$$\|\mathcal{E}(M_\varepsilon)\|_{L^\infty} \leq C_6. \quad (31)$$

Next we estimate

$$\int_0^T \int_{\Omega} |\nabla \mathcal{E}(M_\varepsilon)|^2 dt dx \leq \sup_{r \in [0,1]} \left| \frac{\mathcal{D}(r)}{D(r)} \right| \int_0^T \int_{\Omega} |\nabla \mathcal{D}(M_\varepsilon)|^2 dt dx. \quad (32)$$

By straightforward calculation we verify that because of $a \in (0, 1)$ we have

$$\sup_{r \in [0,1]} \left| \frac{\mathcal{D}(r)}{D(r)} \right| < \infty.$$

In view of (26) and (31)-(32), we obtain that

$$\mathcal{E}(M_\varepsilon) \text{ is bounded in } L^2(0, T; H_0^1(\Omega)). \quad (33)$$

We infer from the continuous embedding of $W^{1,N+1}(\Omega)$ in $L^\infty(\Omega)$ that, for $\varphi \in W^{1,N+1}(\Omega)$ and $t \in (0, T)$,

$$\begin{aligned} & \left| \int_{\Omega} \varphi \partial_t \mathcal{E}(M_\varepsilon)(t) \, dx \right| \\ & \leq \|\partial_t M_\varepsilon(t)\|_{H_0^{-1}(\Omega)} \|\mathcal{D}(M_\varepsilon(t))\varphi\|_{H_0^1(\Omega)} \\ & \leq C_6 \|\partial_t M_\varepsilon(t)\|_{H_0^{-1}(\Omega)} (\|\nabla \mathcal{D}(M_\varepsilon(t))\|_{L^2} + \|\mathcal{D}\|_\infty) \|\varphi\|_{W^{1,N+1}}. \end{aligned}$$

The right-hand side of the above estimate belongs to $L^1(0, T)$ by (27) and (26). This result, along with (33), proves the assertions (29)-(30). Now we are in a position to apply a compactness result [25, Corollary 4] to conclude that $\{\mathcal{E}(M_\varepsilon)\}$ is relatively compact in $L^2((0, T) \times \Omega)$ for each $T > 0$. Thus, for a subsequence (not relabeled) it is convergent almost everywhere in $(0, T) \times \Omega$. Since \mathcal{E} is a monotone function, we deduce that $\{M_\varepsilon\}$ is also convergent almost everywhere. Also, (21), (27) and a classical compactness result [19, Théorème 1.12.1] ensure that $\{M_\varepsilon\}$ is relatively compact in $\mathcal{C}([0, T]; H^{-1}(\Omega))$ for each $T > 0$. Recalling (22) and using the classical compactness argument for the sequence $\{S_\varepsilon\}$, we conclude that there are functions $(S, M) \in L^\infty((0, T) \times \Omega; \mathbb{R}^2)$ and a subsequence of $\{(S_\varepsilon, M_\varepsilon)\}$ (not relabeled) such that

$$(S_\varepsilon, M_\varepsilon) \longrightarrow (S, M) \text{ in } L^2((0, T) \times \Omega; \mathbb{R}^2),$$

and

$$(S_\varepsilon, M_\varepsilon) \longrightarrow (S, M) \text{ in } \mathcal{C}([0, T]; L^2(\Omega)) \times \mathcal{C}([0, T]; H^{-1}(\Omega)).$$

Furthermore, by (26), we infer that $\mathcal{D}(M)$ belongs to $L^2(0, T; H^1(\Omega))$ for each $T > 0$. By the Egorov theorem for any $\delta > 0$, there is a subset $Q_\delta \subset (0, T) \times \Omega$ such that

$$|((0, T) \times \Omega) \setminus Q_\delta| < \delta$$

and $M_\varepsilon \longrightarrow M$ uniformly on Q_δ . Then, (24) entails

$$\mathcal{D}^\varepsilon(M_\varepsilon) \longrightarrow \mathcal{D}(M) \text{ uniformly on } Q_\delta.$$

Hence, for arbitrary $\delta > 0$, we have

$$\mathcal{D}^\varepsilon(M_\varepsilon) \longrightarrow \mathcal{D}(M) \text{ weakly in } L^2(Q_\delta),$$

and we deduce from (23) and (25) that

$$\mathcal{D}^\varepsilon(M_\varepsilon) \longrightarrow \mathcal{D}(M) \text{ weakly in } L^2(0, T; H^1(\Omega)).$$

We are now in a position to pass to the limit in all terms in the weak formulation of (16) and in (28). The classical regularity theory of parabolic equations entails that S is in fact a strong solution satisfying (11) and (13). Thus, (S, M) is a solution to (1)-(3) in the sense of Definition 1.1. \square

To prove the existence of more regular solutions needed for the uniqueness result, let us consider the realization in the space $X = L^q(\Omega)$ of the Laplace operator

$A_q = -\Delta$ with homogeneous Dirichlet boundary condition. Since A_q is a sectorial operator, fractional powers are well defined, and we denote for some $\theta \in (0, 1)$

$$X_q^\theta = D(A_q^\theta),$$

which is a Banach space equipped with the norm (see [24])

$$\|u\|_{X_q^\theta} = \|A_q^\theta u\|_X \quad \text{for } u \in X_q^\theta.$$

We shall use the classical semigroup estimates for the analytic semigroup $e^{-A_q t}$ generated by $-A_q$ (eg. [24, Theorem 6.13 p.74])

$$\|A_q^\theta e^{-A_q t} u\|_X \leq k_\theta t^{-\theta} e^{-at} \|u\|_X \quad (34)$$

which holds for any $u \in X$ for some positive constants k_θ and a . We recall also (cf. [36, Theorem 16.15]) that for Ω with C^2 -boundary

$$X_q^\theta = H_{q,D}^{2\theta}(\Omega) \quad \text{for } 2\theta > \frac{1}{q} \quad (35)$$

where $H_{q,D}^{2\theta}(\Omega)$ is the Bessel potential space of functions satisfying homogeneous Dirichlet boundary condition. Since 2θ is not an integer, $H_{q,D}^{2\theta}(\Omega) = W^{2\theta,q}(\Omega) \cap H_0^1(\Omega)$, where $W^{2\theta,q}(\Omega)$ is the fractional order Sobolev space (Sobolev-Slobodeckii space). Notice also (cf. [29, Theorem 4.6.1(e)]) that for $2\theta > 1 + \frac{N}{q}$

$$H_{q,D}^{2\theta}(\Omega) \subset C^1(\bar{\Omega}). \quad (36)$$

We note also that (cf. [1, Theorem 7.58])

$$W^{2,p}(\Omega) \cap H_0^1(\Omega) \subset W^{2\theta,q}(\Omega) \cap H_0^1(\Omega) \quad \text{for any } p > q. \quad (37)$$

Theorem 2.1. *Assume in addition to the assumptions of Theorem 1.2 that $p > \max(2, N)$ and $S_0 - 1 \in W^{2,p}(\Omega) \cap H_0^1(\Omega)$ and (10) are satisfied. Then there exists a solution to (1)-(3) such that for any $q, p > q > \max(2, N)$ and fixed $T > 0$*

$$S - 1 \in \mathcal{C}([0, T]; X_q^\theta) \cap L^q(0, T; D(A_q)) \cap W^{1,q}(0, T; L^q(\Omega)).$$

Moreover, $v = S - 1$ is a mild solution satisfying

$$v(t) = e^{-At} v_0 + \int_0^t e^{-A(t-s)} F(1 + v(s), M(s)) ds$$

and (13)-(14) are satisfied.

Proof. We first use the regularization (16)-(18) and then the compactness method in a different functional analytic setting than that in Theorem 1.2. Assume that $S_0 \in W^{2,p}(\Omega) \cap H_0^1(\Omega)$ and $M_{0,\varepsilon}$ satisfies (18). Then $v^\varepsilon = S^\varepsilon - 1$ satisfies

$$v^\varepsilon(t) = e^{-At} v_0 + \int_0^t e^{-A(t-s)} F(1 + v^\varepsilon(s), M^\varepsilon(s)) ds. \quad (38)$$

Since for some $C_0 > 0$ we have

$$\|F(1 + v^\varepsilon, M^\varepsilon)\|_{L^\infty(0,T;L^\infty(\Omega))} \leq C_0, \quad (39)$$

uniformly with respect to ε , we deduce from (38) (35), (37) and (34) that there is a constant C' such that

$$\sup_{t \in [0, T]} \|v^\varepsilon(t)\|_{X_q^\theta} \leq C'$$

is satisfied uniformly with respect to ε . Now, similar arguments as in [24, Theorem 3.1 p.74]) combined with (39) and (34) yield

$$\|v^\varepsilon(t)\|_{C^\beta([0,T];X_q^{\theta'})} \leq C''$$

for some $\beta \in (0, 1)$, $C'' > 0$ and θ' such that $\theta < \theta' < 1$ and (35)-(37) are satisfied for θ replaced by θ' . Since Ω is a bounded domain, $X_q^{\theta'}$ is compactly embedded in X_q^θ for $\theta < \theta'$. We use the Arzela-Ascoli Compactness Theorem to conclude that there is a subsequence (not relabeled) such that

$$v^\varepsilon \xrightarrow{\varepsilon \rightarrow 0} v \quad \text{in } \mathcal{C}([0, T]; X_q^\theta).$$

Using the same arguments as in the proof of Theorem 1.2, we may choose a subsequence such that

$$M^\varepsilon \xrightarrow{\varepsilon \rightarrow 0} M \quad \text{in } L^2((0, T); L^2(\Omega)).$$

Therefore, the boundedness and regularity of F entail that

$$F(1 + v^\varepsilon, M^\varepsilon) \xrightarrow{\varepsilon \rightarrow 0} F(1 + v, M) \quad \text{in } L^q(0, T); L^q(\Omega).$$

On passing to the limit in (38), we obtain the mild solution $v \in \mathcal{C}([0, T]; X_q^\theta)$. By the theory of maximal regularity for parabolic equations (cf. [4, Theorem 2.1]), we infer that in fact

$$v \in L^q(0, T; D(A_q)) \cap W^{1,q}(0, T; L^q(\Omega)), \quad (40)$$

provided $v_0 \in W^{2-\frac{2}{q}, q}(\Omega)$. The latter condition is satisfied in our case since $W^{2,p}(\Omega) \subset W^{2-\frac{2}{q}, q}(\Omega)$. By obvious embedding, (40) holds also for $q = 2$, whence $S = v + 1$ satisfies (11) and (13), and it is also an L^2 -weak solution to (1). At last, we notice that by the same reasons as in the proof of Theorem 1.2, M satisfies (12) and (14), which completes the proof. \square

2.2. Uniqueness. The proof of Theorem 1.3 relies on the classical duality technique, which was also used in [18] for the case of chemotaxis equations with a degeneracy of diffusion at the density threshold and no-flux boundary conditions. We note that for the Poisson equation with Dirichlet boundary condition

$$-\Delta u = f \quad \text{in } \Omega, \quad (41)$$

$$u = 0 \quad \text{on } \partial\Omega, \quad (42)$$

given $f \in L^2(\Omega)$, we have $u = (-\Delta)^{-1}f \in H^2(\Omega) \cap H_0^1(\Omega)$. It follows that $\varphi = (-\Delta)^{-1}f$ is a suitable test function in (14).

To shorten notation, we denote

$$h_{\sigma_1, \sigma_2}(M) := d_{22} M^{\sigma_1} (1 - M)^{\sigma_2}.$$

We shall use the following lemma

Lemma 2.2. *If*

$$\sigma_1 \geq 1 + \frac{b}{2}, \quad \sigma_2 \geq 1 - \frac{a}{2}. \quad (43)$$

then there exists a constant $C_0 > 1$ such that

$$(h_{\sigma_1, \sigma_2}(u) - h_{\sigma_1, \sigma_2}(v))^2 \leq C_0(u - v)(\mathcal{D}(u) - \mathcal{D}(v))$$

for any $u, v \in [0, 1]$.

Proof. Using (43) and the Cauchy-Schwarz inequality, we obtain

$$\begin{aligned}
h_{\sigma_1, \sigma_2}(u) - h_{\sigma_1, \sigma_2}(v) &= \int_v^u h'_{\sigma_1, \sigma_2}(s) ds \\
&\leq |\sigma_1 + \sigma_2| \int_v^u \frac{s^{\sigma_1-1}(1-s)^{\sigma_2-1}}{D^{1/2}(s)} D(s)^{1/2} ds \\
&\leq |\sigma_1 + \sigma_2| \sup_{s \in [0,1]} \{s^{\sigma_1-1-b/2}(1-s)^{\sigma_2-1+a/2}\} \int_v^u D(s)^{1/2} ds \\
&\leq C(a, b, \sigma_2, \sigma_1)(u-v)^{1/2}((\mathcal{D}(u) - \mathcal{D}(v))^{1/2})
\end{aligned}$$

where $C(a, b, \sigma_1, \sigma_2)$ is a constant. Finally we set $C_0 = \sqrt{C(a, b, \sigma_1, \sigma_2)} + 1$. \square

Proof of Theorem 1.3. Let (S, M) and (\hat{S}, \hat{M}) be two solutions to (1)-(3) in the sense of Definition 1.1 and fix $T > 0$. We set

$$V(t, x) := S(t, x) - \hat{S}(t, x), \quad U(t, x) := M(t, x) - \hat{M}(t, x),$$

in $[0, T] \times \Omega$. In light of (5) and (7) and the regularity of functions g, f_1, f_2 , there exists a constant $L > 0$ such that for any $0 \leq S, \hat{S}, M, \hat{M} \leq 1$

$$|F(S, M) - F(\hat{S}, \hat{M})| \leq L(|V| + |U|), \quad (44)$$

$$|G(S, M) - G(\hat{S}, \hat{M})| \leq L(|h_{\alpha, \beta}(M) - h_{\alpha, \beta}(\hat{M})| + |S - \hat{S}|), \quad (45)$$

Notice that U satisfies

$$\begin{aligned}
\int_0^t \langle \partial_t U, \psi \rangle ds &= \int_0^t \int_{\Omega} - \left[\nabla \left(\mathcal{D}(M) - \mathcal{D}(\hat{M}) \right) \right. \\
&\quad \left. - \left(h_{d,c}(M) - h_{d,c}(\hat{M}) \right) \nabla S - h_{d,c}(\hat{M}) \nabla V \right] \cdot \nabla \psi \, dx ds \\
&\quad + \int_0^t \int_{\Omega} \left(G(S, M) - G(\hat{S}, \hat{M}) \right) \psi \, dx ds
\end{aligned} \quad (46)$$

for each $\psi \in L^2(0, t; H_0^1(\Omega))$. Taking $\psi = (-\Delta)^{-1}U$ in (46) we obtain

$$\begin{aligned}
\int_{\Omega} |\nabla(-\Delta)^{-1}U(t)|^2 dx &= \int_{\Omega} |\nabla(-\Delta)^{-1}U(0)|^2 dx + 2 \int_0^t \langle \partial_t U, (-\Delta)^{-1}U \rangle ds \\
&= 2 \int_0^t \int_{\Omega} \Delta(-\Delta)^{-1}U \left(\mathcal{D}(M) - \mathcal{D}(\hat{M}) \right) dx ds \\
&\quad + 2 \int_0^t \int_{\Omega} \left(h_{d,c}(M) - h_{d,c}(\hat{M}) \right) \nabla(-\Delta)^{-1}U \cdot \nabla S \, dx ds \\
&\quad + 2 \int_0^t \int_{\Omega} h_{d,c}(\hat{M}) \nabla(-\Delta)^{-1}U \cdot \nabla V \, dx ds \\
&\quad + 2 \int_0^t \int_{\Omega} \left(G(S, M) - G(\hat{S}, \hat{M}) \right) (-\Delta)^{-1}U \, dx ds.
\end{aligned}$$

To find a bound for the last integral, we use the Poincaré inequality with a constant C_P (see e.g. [27, Theorem 11.11]). Then, using (44) (45) and the Young inequality,

we obtain for each $\delta > 0$ that

$$\begin{aligned}
& \int_{\Omega} |\nabla(-\Delta)^{-1}U(t)|^2 dx \\
& \leq -2 \int_0^t \int_{\Omega} (M - \hat{M}) \left(\mathcal{D}(M) - \mathcal{D}(\hat{M}) \right) dx ds \\
& \quad + 2 \int_0^t \|\nabla S\|_{L^\infty} \|\nabla(-\Delta)^{-1}U\|_{L^2} \|h_{d,c}(M) - h_{d,c}(\hat{M})\|_{L^2} ds \\
& \quad + 2 \|h_{d,c}\|_{L^\infty(0,1)} \int_0^t \|\nabla(-\Delta)^{-1}U\|_{L^2} \|\nabla V\|_{L^2} ds \\
& \quad + 2 \int_0^t L(\|V\|_{L^2} + \|h_{\alpha,\beta}(M) - h_{\alpha,\beta}(\hat{M})\|_{L^2}) \|(-\Delta)^{-1}U\|_{L^2} ds \\
& \leq -2 \int_0^t \int_{\Omega} (M - \hat{M}) \left(\mathcal{D}(M) - \mathcal{D}(\hat{M}) \right) dx ds \\
& \quad + \delta \int_0^t \int_{\Omega} [(h_{d,c}(M) - h_{d,c}(\hat{M}))^2 + (h_{\alpha,\beta}(M) - h_{\alpha,\beta}(\hat{M}))^2] dx ds \\
& \quad + \frac{1}{\delta} \int_0^t \|\nabla S\|_{L^\infty}^2 \|\nabla(-\Delta)^{-1}U\|_{L^2}^2 ds \\
& \quad + \delta \int_0^t \|\nabla V\|_{L^2}^2 ds + \frac{\|h_{d,c}\|_{L^\infty(0,1)}^2}{\delta} \int_0^t \|\nabla(-\Delta)^{-1}U\|_{L^2}^2 ds \\
& \quad + \delta \int_0^t \|V\|_{L^2}^2 ds + \frac{L^2 C_P}{\delta} \int_0^t \|\nabla(-\Delta)^{-1}U\|_{L^2}^2 ds.
\end{aligned}$$

Since $\nabla S \in L^\infty(0, T; L^\infty(\Omega))$ (this is a consequence of Theorem 2.1 and the embeddings (35),(36)), we obtain the further estimate

$$\begin{aligned}
& \int_{\Omega} |\nabla(-\Delta)^{-1}U(t)|^2 dx \\
& \leq \int_0^t \int_{\Omega} \{-2(M - \hat{M})(\mathcal{D}(M) - \mathcal{D}(\hat{M})) \\
& \quad + \delta((h_{d,c}(M) - h_{d,c}(\hat{M}))^2 + (h_{\alpha,\beta}(M) - h_{\alpha,\beta}(\hat{M}))^2)\} dx ds \\
& \quad + \frac{\|h_{d,c}\|_{L^\infty(0,1)}^2 + L^2 C_P + \|\nabla S\|_{L^\infty(0,T;L^\infty(\Omega))}^2}{\delta} \int_0^t \|\nabla(-\Delta)^{-1}U\|_{L^2}^2 ds \\
& \quad + \delta \int_0^t \|V\|_{L^2}^2 + \|\nabla V\|_{L^2}^2 ds.
\end{aligned}$$

With Lemma 2.2 and $\delta < \frac{1}{C_0}$, we obtain

$$\begin{aligned}
& \int_{\Omega} |\nabla(-\Delta)^{-1}U(t)|^2 dx \\
& \leq \delta \left(\int_0^t \|V\|_{L^2}^2 + \|\nabla V\|_{L^2}^2 ds \right) + C_1(T) \int_0^t \|\nabla(-\Delta)^{-1}U\|_{L^2}^2 ds, \tag{47}
\end{aligned}$$

where $C_1(T)$ is a constant depending on $\|h\|_{L^\infty(0,1)}$, L , C_P and $\|\nabla S\|_{L^\infty(0,T;L^\infty(\Omega))}$. It next follows from (2), (6) and the boundedness of \hat{M} , S and \hat{S} on $(0, T) \times \Omega$ that

$$\begin{aligned} & \frac{1}{2} \frac{d}{dt} \|V\|_{L^2}^2 + d_1 \|\nabla V\|_{L^2}^2 = \\ & \int_{\Omega} V \left((f_1(S) - f_1(\hat{S})) + \hat{M} (f_2(S) - f_2(\hat{S})) \right) dx + \int_{\Omega} f_2(S) U V dx \\ & \leq \|(\hat{M}\|_{\infty} + 1)L\|V\|_{L^2}^2 + \int_{\Omega} \nabla(-\Delta)^{-1}U \cdot \nabla(f_2(S) V) dx \\ & \leq \frac{d_1}{2} \|\nabla V\|_{L^2}^2 + C_2(T) (\|V\|_{L^2}^2 + (1 + \|\nabla S\|_{L^\infty}^2) \|\nabla(-\Delta)^{-1}U\|_{L^2}^2), \end{aligned}$$

where we have used (41)-(42) with f replaced by U , and $C_2(T)$ is a constant depending on the data. It follows that

$$\begin{aligned} & \|V(t)\|_{L^2}^2 + \frac{d_1}{2} \int_0^t \|\nabla V\|_{L^2}^2 ds \\ & \leq C_2(T) \int_0^t (\|V\|_{L^2}^2 + (1 + \|\nabla S\|_{L^\infty}^2) \|\nabla(-\Delta)^{-1}U\|_{L^2}^2) ds. \end{aligned}$$

Next, we add the above inequality and (47) for $\delta \leq \min\{d_1/4, 1/C_0\}$. We deduce that

$$\begin{aligned} & \|V(t)\|_{L^2}^2 + \|\nabla(-\Delta)^{-1}U(t)\|_{L^2}^2 \\ & \leq C_3(T) \int_0^t (1 + \|\nabla S\|_{L^\infty}^2) (\|V\|_{L^2}^2 + \|\nabla(-\Delta)^{-1}U\|_{L^2}^2) ds. \end{aligned}$$

Since $\nabla S \in L^\infty(0, T; L^\infty(\Omega))$ by Theorem 2.1, we finally use the Gronwall lemma to obtain that $V(t) = \nabla(-\Delta)^{-1}U(t) = 0$ for every $t \in [0, T]$, which completes the proof. \square

3. Numerical simulations. Although the model (1)-(2) is formulated for a general three-dimensional setting, we restrict our simulations to the one-dimensional case, for computational convenience and to allow a more straightforward presentation and discussion of the simulation results. The goal of our simulation study will be to investigate the potential effect of chemotaxis in early stages of biofilm colony formation, for a generic biofilm rather than a particular biological system. We will do this by comparing simulations of the biofilm-chemotaxis model with the simulations of the corresponding biofilm model without chemotaxis.

We simulate the model in a domain of length $L = 0.5mm$. For the reaction part, we use the functions $F(S, M)$ and $G(S, M)$ in (8) and (9). The parameters a, b, c, d that describe the spatial movement of biomass and the new growth parameters α, β are chosen in accordance with Theorem 1.3, to ensure existence of a unique solution. The remaining growth kinetics parameters and the substrate diffusion coefficient are taken from Benchmark Problem 1 of the International Water Association's Taskgroup on Biofilm Modeling [32], where the maximum uptake rate k_1 in (8) is compounded from the maximum specific growth rate k_3 , a yield coefficient and the maximum cell density. The half saturation concentration k_2 is chosen clearly smaller than unity, i.e. we consider the case of biomass growth that is not initially substrate limited. These parameters are kept constant for all simulations. The biomass motility parameters d_{21} and d_{22} are varied to investigate different scenarios. All model parameters are collected in Table 1.

TABLE 1. Model parameters used in the simulations

parameter	symbol	value	unit
system length	L	$5 \cdot 10^{-4}$	m
substrate diffusion coefficient	d_1	10^4	$m^2 d^{-1}$
biomass motility coefficient (diffusion)	d_{21}	<i>varied</i>	$m^2 d^{-1}$
biomass motility coefficient (chemotaxis)	d_{22}	<i>varied</i>	$m^2 d^{-1}$
maximum substrate uptake rate	k_1	95238.1	d^{-1}
half saturation concentration	k_2	0.2	–
maximum growth rate	k_3	6	d^{-1}
biomass diffusion exponent	a	0.5	–
biomass diffusion exponent	b	4	–
chemotaxis exponent	c	3	–
chemotaxis exponent	d	3	–
logistic growth exponent	α	3	–
logistic growth exponent	β	0.8	–

The numerical method that we use in these simulations is a straightforward adaptation of the semi-implicit Finite Volume Method [6] for the density-dependent diffusion-reaction biofilm model. This method is able to deal with both the degeneracy and the singularity in the biomass diffusion equation with sufficient accuracy, while requiring only moderate spatial refinement [6, 22]; in our simulations we use 200 grid points. In the numerical treatment the additional chemotaxis terms in (2) are treated as convective terms with density dependent convective velocity.

The system which we simulate corresponds to a standard biofilm growth scenario. We start with initial data with compact support. The region where $M = 0$ is the aqueous phase, the region with $M > 0$ is the actual biofilm. Due to growth, both regions change in time. We use the initial data

$$S_0 = 1 \quad \text{and} \quad M_0(x) = \begin{cases} m_0 & \frac{L}{2} - r \leq x \leq \frac{L}{2} + r \\ 0 & \text{else} \end{cases} \quad (48)$$

with $r = 0.05 * L$.

It is easy to verify that these symmetric initial data will lead to a symmetric solution, which is unique if the conditions of Theorem 1.3 are met. This solution will have $M_x = S_x = 0$ for $x = L/2$. Therefore the solution of the problem restricted to the interval $0 < x < L/2$ can be interpreted as the solution of the system with a biofilm originally in a small pocket on a impermeable substratum at $L/2$. When we present and discuss the solution we will, therefore, restrict ourselves to the interval $0 < x < L/2$.

The nutrients are added into the system at $x = 0$, due to (4), i.e. at the boundary on the opposite side of the substratum. Thus chemotaxis is expected to lead to a faster expansion of the biofilm toward the nutrient source. A particularity, or artefact, of the Dirichlet boundary conditions is that by virtue of the maximum principle, a higher amount of biomass leads to steeper substrate gradients at the boundary, i.e. to improved environmental conditions.

In Figure 1 we plot the solution $S(t, x)$, $M(t, x)$ of (1), (2), (4), (48) for biomass motility coefficients $d_{21} = d_{22} = 10^{-12}$ as surface data over the x - t -plane. In the beginning, biomass growth is very slow and appears to be almost stationary. After some time biomass density in the biofilm pocket starts increasing without the biofilm

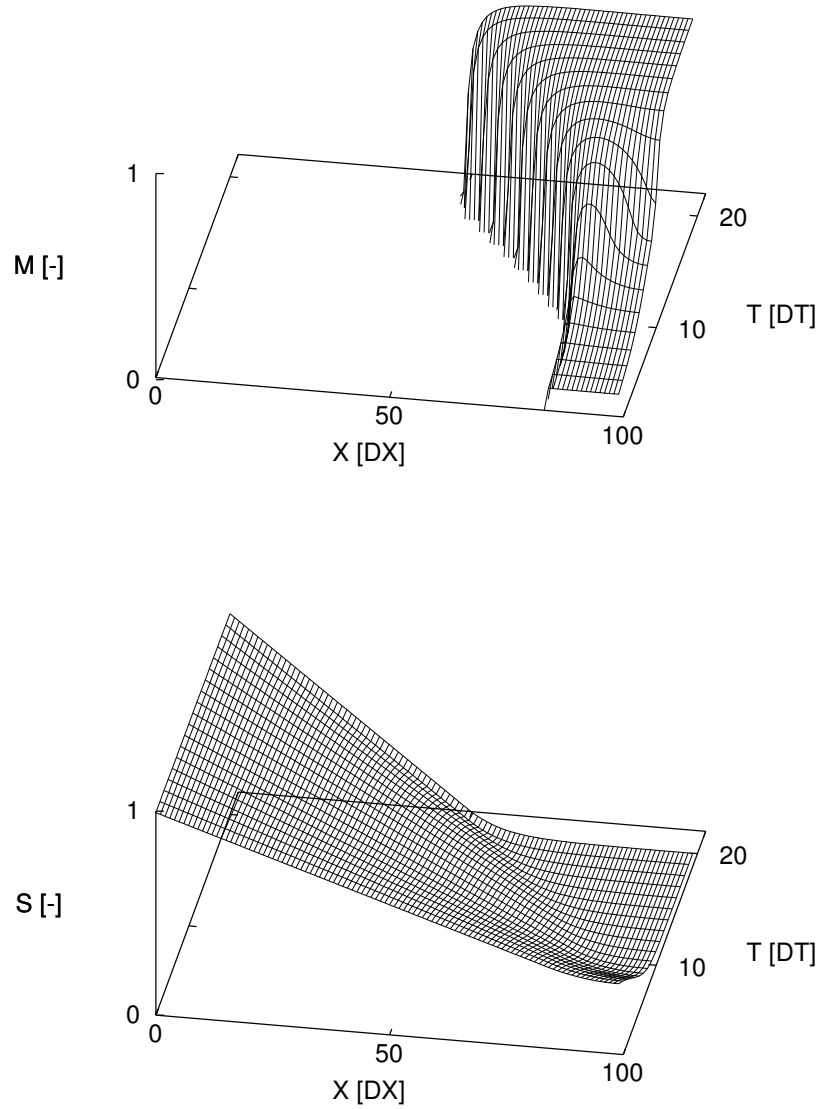


FIGURE 1. Biomass density $M(t, x)$ (top panel) and substrate concentration $S(t, x)$ (bottom panel) as a solution of (1), (2), (4), (48) with parameters according to Table 1 and biomass motility coefficients $d_{21} = d_{22} = 10^{-10}$. The units in x direction are grid point spacings $\Delta x = L/200$, the units in t direction are output timesteps $\Delta T = 2d$.

region expanding. Initially the biomass density increases faster in the outer layer of the biofilm (close to the biofilm/aqueous phase interface) than in the inner layer (at the substratum), due to higher nutrient availability and no pressure to diffuse. Once the biomass density reaches values close to unity, the biofilm region starts expanding and the biomass density attains a value $M \approx 1$ in the interior of the biofilm. The substrate concentration field coincides with the biomass density. It attains its minimum at the substratum. The more biomass there is in the system the lower is the substrate concentration. The substrate gradient at the boundary $x = 0$ increases as biomass grows.

In order to assess the contribution of chemotaxis to biomass movement, relative to diffusion, we plot in Figure 2 and Figure 3 the biomass densities for various choices of the biomass motility coefficients. Together with the solution of our original model (2) with $d_{21} > 0$, $d_{22} > 0$ we plot the solution of the corresponding biofilm model without chemotaxis-term ($d_{21} > 0$, $d_{22} = 0$), i.e. the solution of

$$\partial_t M = \nabla \cdot \left(d_{21} \frac{M^b}{(1-M)^a} \nabla M \right) + G(S, M).$$

In Figure 2 we show simulations of the model with the same biomass motility coefficient for both processes, diffusion and chemotaxis, i.e. $d_{21} = d_{22}$. These parameters range here from 10^{-12} to 10^{-8} . The left column of Figure 2 contains the plots of M for the model with diffusion and chemotaxis, the right column contains the solution for the model with diffusion only. The biomass motility coefficient d_{21} controls how fast the biofilm region expands and to which maximum biomass density it grows. For $d_{21} = 10^{-12}$, expansion is very slow and the biomass density reaches values close to $M \approx 1$ inside the biofilm (Figure 2.a). For $d_{21} = 10^{-10}$ the biofilm expands faster, still growing close to maximum cell density (Figure 2.b). For the largest value, the biofilm expands quickly, but does not exceed values of $M \approx 0.6$ (Figure 2.c). This choice of parameters is therefore considered too big to be realistic. In the cases of Figure 2.a,b, the solution of the model with and without chemotaxis are virtually indistinguishable, indicating that chemotaxis does not contribute noteworthy to biofilm formation in such cases. In the case of the higher values $d_{21} = d_{22} = 10^{-8}$ for the biomass motility coefficients we observe differences in M , see Figure 2.c. Including chemotactic effects leads to a faster growing biofilm structure; albeit with lower biomass density.

In Figure 3, we use different biomass motility coefficients d_{21}, d_{22} . In all cases we choose the chemotactic motility coefficient to be higher than the diffusive one, $d_{21} \ll d_{22}$. Again, the solution of the diffusion-chemotaxis model is shown in the left column, the solution of the model with diffusion only in the right column. We notice distinct differences in the biomass densities of the models with and without chemotaxis, in the cases of Figure 3.a,c, where $d_{22} = 10^{-8}$ but not so in Figure 3.b, where $d_{22} = 10^{-10}$. In the case of Figure 3.a, with $d_{21} = 10^{-12}$ and $d_{22} = 10^{-8}$ chemotaxis leads to a very different biofilm structure than obtained by the model without chemotaxis. The chemotactic effect pulls biomass toward the nutrient source and leads to a biofilm that is much denser close to the biofilm/water interface than in the inner layers close to the substratum. This could be understood as the 1D analogy of mushroom type biofilm colonies in 2D/3D. In the case of Figure 3.c, with $d_{21} = 10^{-10}$ and $d_{22} = 10^{-8}$, on the other hand the differences are not as pronounced, yet clearly visible. Interestingly, it appears that the biofilm without chemotaxis grows bigger and denser in this case than the one with chemotaxis. The

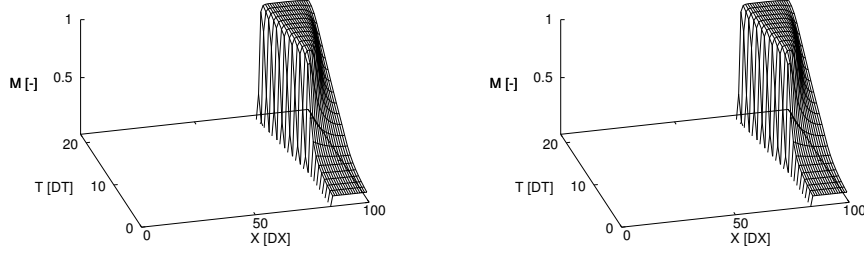
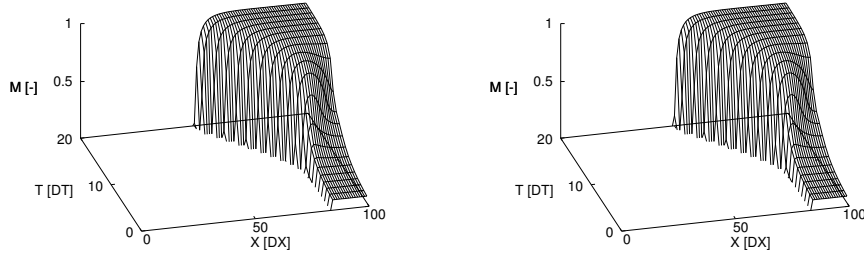
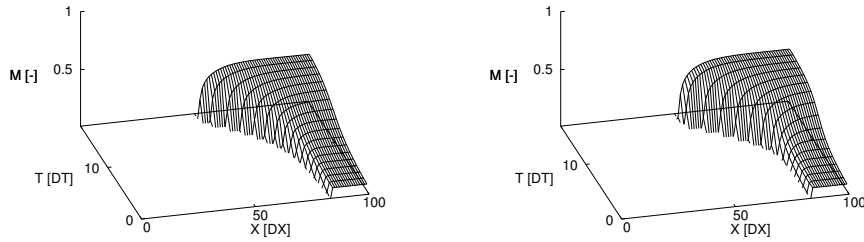
(a) $d_{21} = d_{22} = 10^{-12}$ (b) $d_{21} = d_{22} = 10^{-10}$ (c) $d_{21} = d_{22} = 10^{-8}$

FIGURE 2. Comparison of the chemotaxis-diffusion biofilm model (left column) with the diffusion-only biofilm model (right column). Plotted are biomass densities $M(t, x)$ for various biomass motility coefficients for the case $d_{21} = d_{11}$. The units in x direction are grid point spacings $\Delta x = L/200$, the units in t direction are output timesteps $\Delta T = 2d$.

substrate concentration $S(t, x)$ in all cases is similar as shown in Figure 1; these data are omitted.

These simulations were repeated several times with different exponents of the chemotaxis model, and with different initial data (smaller initial inoculum, or non-constant biomass distribution in the inoculum). In all cases the results were qualitatively the same (data not shown). This suggests that early stages chemotaxis will only affect biofilm structure quantitatively if the biomass motility coefficient

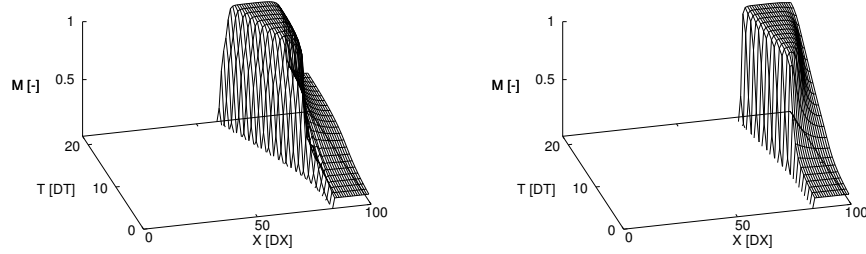
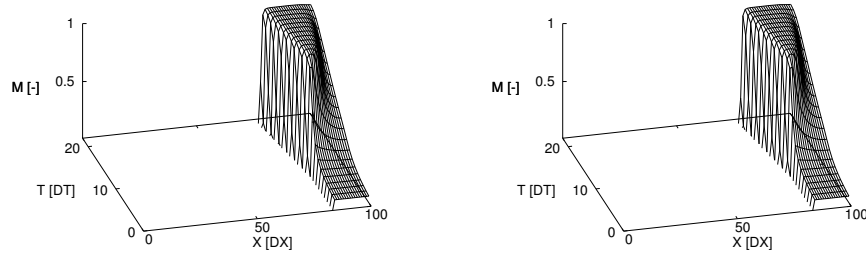
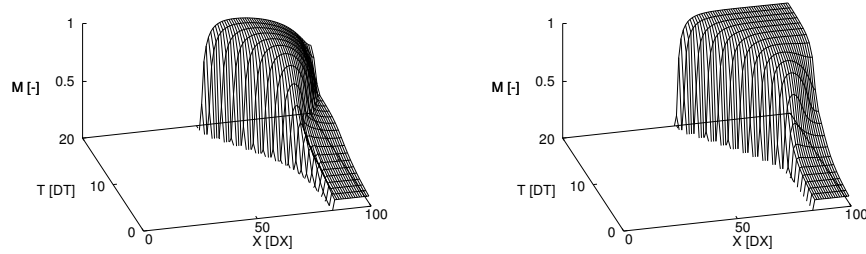
(a) $d_{21} = 10^{-12}, d_{22} = 10^{-8}$ (b) $d_{21} = 10^{-12}, d_{22} = 10^{-10}$ (c) $d_{21} = 10^{-10}, d_{22} = 10^{-8}$

FIGURE 3. Comparison of the chemotaxis-diffusion biofilm model (left column) with the diffusion-only biofilm model (right column), continued. Plotted are biomass densities $M(t, x)$ for various biomass motility coefficients for the case $d_{21} < d_{22}$. The units in x direction are grid point spacings $\Delta x = L/200$, the units in t direction are output timesteps $\Delta T = 2d$.

due to chemotaxis is substantially larger than the biomass motility coefficient due to diffusive biomass spreading. In the simulations presented here it was required that $d_{22} = 10^{-8}$ in order to observe notable effects. It is reasonable to assume that this parameter depends on the material properties of the particular biofilm (species and environment), in particular of the EPS, in which cells are embedded, but also parameters that describe the ability of the cells to move, e.g. by flagellar motion or twitching motility.

4. Conclusion. We presented and analysed a qualitative model for the initial formation of bacterial biofilms, with focus on early stages where chemotaxis could potentially make a contribution to biofilm development. The model equation for biomass includes degenerate and singular diffusion effects in biomass spreading, as well as a nonlinear extension of the Keller-Segel chemotaxis model. We found conditions on diffusion and chemotaxis parameters for which the existence of a unique (weak) solution can be established.

The first numerical simulations of the model that we conducted remained in some sense as inconclusive as many experimental studies of chemotaxis effects in biofilms. In particular our results indicate that whether or not chemotactic effects affect biofilm formation might largely depend on the biomass motility coefficients due to (nonlinear) diffusion and due to chemotaxis. The latter might depend on the species and on the particular environment.

The model investigated here provides merely a mathematical framework to study the interplay of biofilm-style combined degenerate and fast diffusion with degenerate chemotaxis terms, but it is not tailored to a particular biological system. In fact the system studied here is the simplest representative and should be considered primarily a study of proof of mathematical concept. Of particular interest would be to apply this concept to study biofilm formation in chemotactic response to signals received from the substratum. This, however, requires an extension of the theory developed here to a set of nonlinear Robin boundary conditions and to include additional biofilm constituents.

Acknowledgments. We express our gratitude to the referees. Their remarks and suggestions helped to improve the paper.

D.W. would like to thank the Helmholtz Zentrum Munich for financial support during his stay in April, 2011. His work was also supported by the Polish Ministry of Science and Higher Education under the grant N201547638. H.J.E. was supported in parts by the Natural Science and Engineering Research Council of Canada with a Discovery Grant. A.Z. was supported by The Elite Network of Bavaria.

REFERENCES

- [1] R. Adams, “Sobolev Spaces,” Pure and Applied Mathematics, Vol. 65, Academic Press [A subsidiary of Harcourt Brace Jovanovich, Publishers], New York-London, 1975.
- [2] H. Amann, *Nonhomogeneous linear and quasilinear elliptic and parabolic boundary value problems*, in “Function Spaces, Differential Operators and Nonlinear Analysis” (eds. H. Triebel and H. J. Schmeisser), Teubner-Texte Math., **133**, Teubner, Stuttgart, (1993), 9–126.
- [3] D. G. Aronson, *The porous medium equation*, in “Nonlinear Diffusion Problems” (Montecatini Terme, 1985), Lecture Notes in Mathematics, **1224**, Springer, Berlin, 1986.
- [4] R. Denk, M. Hieber and J. Prüss, *Optimal $L^p - L^q$ -estimates for parabolic boundary value problems with inhomogeneous data*, Math. Z., **257** (2007), 193–224.
- [5] J. Dockery and I. Klapper, *Finger formation in biofilm layers*, SIAM J. Appl. Math., **62** (2001/02), 853–869.
- [6] H. J. Eberl and L. Demaret, *A finite difference scheme for a degenerated diffusion equation arising in microbial ecology*, in “Proceedings of the Sixth Mississippi State–UBA Conference on Differential Equations and Computational Simulations,” El. J. Diff Equs Conf., **15**, Southwest Texas State Univ., San Marcos, TX, (2007), 77–96.
- [7] H. J. Eberl, D. F. Parker and M. C. M. Van Loosdrecht, *A new deterministic spatio-temporal continuum model for biofilm development*, J. Theor. Med., **3** (2001), 161–176.
- [8] M. A. Efendiev and S. Sonner, *Verifying mathematical models with diffusion, transport and interaction*, in “Current Advances in Nonlinear Analysis and Related Topics,” GAKUTO Internat. Ser. Math. Sci. Appl., **32**, Gakkōtoshō, Tokyo, (2010), 41–67.

- [9] M. A. Efendiev, R. Lasser and S. Sonner, *Necessary and sufficient conditions for an infinite system of parabolic equations preserving the positive cone*, Int. J. Biomath. & Biostats, **1** (2010), 47–52.
- [10] M. A. Efendiev, S. V. Zelik and H. J. Eberl, *Existence and long time behaviour of a biofilm model*, Comm. Pure and Appl. Analysis, **8** (2009), 509–531.
- [11] M. A. Efendiev and T. Senba, *On the well-posedness of a class of PDEs including porous medium and chemotaxis effect*, Adv. Differ. Equ., **16** (2011), 937–954.
- [12] M. A. Efendiev and A. Zhigun, *On a 'balance' condition for a class of PDEs including porous medium and chemotaxis effect: Non-autonomous case*, Adv. Math. Sci. Appl., **21** (2011), 285–304.
- [13] H. Fgaier, B. Feher, R. C. McKellar and H. J. Eberl, *Predictive modeling of siderophore production by Pseudomonas fluorescens under iron limitation*, J. Theor. Biol., **251** (2008), 348–362.
- [14] H. Fgaier and H. J. Eberl, *Parameter identification and quantitative comparison of differential equations that describe physiological adaptation of a bacterial population under iron limitation*, Disc. Cont. Dyn. Sys. Suppl., (2009), 230–239.
- [15] M. R. Frederick, C. Kuttler, B. A. Hense, J. Müller and H. J. Eberl, *A mathematical model of quorum sensing in patchy biofilm communities with slow background flow*, Can. Appl. Math. Quart., **18** (2011), 267–298.
- [16] R. Kowalczyk, A. Gamba and L. Preciosi, *On the stability of homogeneous solutions to some aggregation models*, Discrete Contin. Dynam. Systems-Series B, **4** (2004), 203–220.
- [17] V. Gordon, *Personal email communication*, July 4, (2011).
- [18] Ph. Laurençot and D. Wrzosek, *A chemotaxis model with threshold density and degenerate diffusion*, in “Nonlinear Elliptic and Parabolic Problems,” Progr. Nonlinear Differential Equations Appl., **64**, Birkhäuser, Basel, (2005), 273–290.
- [19] J.-L. Lions, “Quelques Méthodes de Résolution des Problèmes aux Limites non Linéaires,” Dunod; Gauthier-Villars, Paris, 1969.
- [20] P. M. Lushnikov, N. Chen and M. Alber, *Macroscopic dynamics of biological cells interacting via chemotaxis and direct contact*, Phys. Rev. E., **78** (2008), 061904, 12 pp.
- [21] M. A. Molina, J.-L. Ramos and M. Espinosa-Urgel, *Plant-associated biofilms*, Rev. Environ. Sci. Biotech., **2** (2003), 99–108.
- [22] N. Muhammad and H. J. Eberl, *Model parameter uncertainties in a dual-species biofilm competition model affect ecological output parameters much stronger than morphological ones*, Math. Biosci., **233** (2011), 1–18.
- [23] K. Painter and T. Hillen, *Volume-filling and quorum-sensing in models for chemosensitive movement*, Can. Appl. Math. Quart., **10** (2002), 501–543.
- [24] A. Pazy, “Semigroups of Linear Operators and Applications to Partial Differential Equations,” Applied Mathematical Sciences, **44**, Springer-Verlag, New York, 1983.
- [25] J. Simon, *Compact sets in the space $L^p(0, T; B)$* , Ann. Mat. Pura Appl. (4), **146** (1987), 65–96.
- [26] R. Singh, D. Paul and R. K. Jain, *Biofilms: Implications in bioremediation*, TRENDS in Microbiol., **14** (2006), 389–397.
- [27] J. Smoller, “Shock Waves and Reaction-Diffusion Equations,” Second edition, Grundlehren der Mathematischen Wissenschaften [Fundamental Principles of Mathematical Sciences], **258**, Springer-Verlag, New York, 1994.
- [28] Y. Sugiyama and H. Kunii, *Global existence and decay properties for a degenerate Keller-Segel model with a power factor in drift term*, J. Diff. Equ., **227** (2006), 333–364.
- [29] H. Triebel, “Interpolation Theory, Function Spaces, Differential Operators,” North-Holland Mathematical Library, **18**, North-Holland Publishing Co., Amsterdam-New York, 1978.
- [30] Z. A. Wang, M. Winkler and D. Wrzosek, *Singularity formation in chemotaxis systems with volume-filling effect*, Nonlinearity, **24** (2011), 3279–3297.
- [31] Z. A. Wang, M. Winkler and D. Wrzosek, *Global regularity vs. infinite-time singularity formation in a chemotaxis model with volume filling effect and degenerate diffusion*, SIAM J. Math. Anal., **44** (2012), 3502–3525.
- [32] O. Wanner, H. Eberl, E. Morgenroth, D. Noguera, C. Picioreanu, B. Rittmann and M. van Loosdrecht, “Mathematical Modeling of Biofilms,” IWA Publishing, London, 2006.
- [33] D. Wrzosek, *Chemotaxis models with a threshold cell density*, in “Parabolic and Navier-Stokes Equations. Part 2,” Banach Center Publ., **81**, Polish Acad. Sci. Inst. Math., Warsaw, (2008), 553–566.

- [34] D. Wrzosek, *Model of chemotaxis with threshold density and singular diffusion*, Nonl. Analysis TMA, **73** (2010), 338–349.
- [35] D. Wrzosek, *Volume filling effect in modelling chemotaxis*, Math. Model. Nat. Phenom., **5** (2010), 123–147.
- [36] A. Yagi, “Abstract Parabolic Evolution Equations and their Applications,” Springer Monographs in Mathematics, Springer-Verlag, Berlin, 2010.
- [37] P. M. Yaryura, M. León, O. S. Correa, N. L. Kerber, N. L. Pucheu and A. F. García, *Assessment of the role of chemotaxis and biofilm formation as requirement for colonization of roots and seed of soybean plants by Bacillus amyloliquifaciens BNM339*, Curr. Microbiol., **56** (2008), 625–632.

Received October 2012; revised March 2013.

E-mail address: heberl@uoguelph.ca

E-mail address: messoud.efendiyev@helmholtz-muenchen.de

E-mail address: D.Wrzosek@mimuw.edu.pl

E-mail address: zhigun@ma.tum.de